

An intercomparison study of TSM, SEBS and SEBAL using high resolution imagery and Lysimetric data

George Paul¹, Prasanna H. Gowda², P.V. Vara Prasad¹, Terry A. Howell², Scott A. Staggenborg¹, Paul D. Colaizzi², Stacy L. Hutchinson³, Robert M. Aiken¹
¹Agronomy, Kansas State University; ²USDA-ARS-Conservation and Production Research Lab, Texas; ³ Biological and Agricultural Engineering, Kansas State University

INTRODUCTION

Evapotranspiration (ET) mapping has many applications including crop water management, climate change impact assessment, hydrological modeling, groundwater recharge studies, irrigation performance, and land use planning. Satellite-based thermal infrared remote sensing has greatly contributed to the development and improvement of remote sensing-based evapotranspiration (RS-ET) mapping algorithms. Testing and validation of RS-ET algorithms across a range of hydrometeorological and surface cover conditions is important to fill in the existing gap in the operationalization of these algorithms. The primary objective of this research was to test and improve three widely used RS-ET models. Three algorithms evaluated in this study include: SEBAL (Surface Energy Balance Algorithm for Land), SEBS (Surface Energy Balance System) and TSM (Two Source Energy Balance Model).

THEORY

SEBAL, SEBS, and TSM utilize the Monin-Obukhov similarity (MOS) theory to solve for the sensible heat and calculate ET as the residual of the surface energy balance (Net Radiation = Soil Heat Flux + Sensible Heat Flux + Latent Heat Flux). In general, the residual surface energy balance scheme can be categorized into single-source (SEBS and SEBAL) and dual-source (TSM) model, differing in their treatment of soil and vegetation source contribution as composite or distributed, respectively. Below is the bulk formulation of sensible heat (H) based on the gradient-resistance relation as defined by each of the three algorithms.

SEBAL	SEBS	TSM
$H = \rho_a C_p \frac{dT_{1,2}}{r_{ah,1,2}}$	$H = \rho_a C_p \frac{\theta_0 - \theta_a}{r_{ah}}$	$H_C = \rho_a C_p \frac{T_C - T_{AC}}{r_x}$ $H_S = \rho_a C_p \frac{T_S - T_{AC}}{r_s}$ $H = \rho_a C_p \frac{T_{AC} - T_A}{r_a}$
<p>where ρ_a is air density (kg m^{-3}), C_p is specific heat of air at constant pressure ($\text{J kg}^{-1} \text{K}^{-1}$) and $r_{ah,1,2}$ is aerodynamic resistance (sm^{-1}) between two near-surface heights, z_1 and z_2 taken as 0.1 and 2 m. The dT parameter (K) represents the near-surface temperature difference between z_1 and z_2.</p> <p>Pitfall: The parameter dT is assumed to be a linear function of radiometric surface temperature across the study region. The dT function is derived from two point known as the hot and cold pixel whose selection is highly subjective to analysts' decision.</p>	<p>where θ_0 is the potential surface temperature and θ_a is the potential air temperature. The aerodynamic resistance r_{ah}, is defined as the resistance from height $z_{oh} + d_0$ (d_0 is zero plane displacement height, and z_{oh} (m) is roughness length for heat transport) having an aerodynamic temperature, to the height z_{ref}. z_{oh} is related to an excess resistance parameter kB^{-1}.</p> <p>Pitfall: Highly sensitive to the air temperature input data.</p>	<p>where H_C, H_S and H are the sensible heat for canopy, soil and total. T_C, T_A, T_S, and T_{AC} are the temperatures of the canopy, air, soil and air temperature within the canopy boundary layer. r_x is the resistance in the boundary layer near the canopy, r_s is the resistance to heat flux in the boundary layer immediately above the soil surface and r_a is the aerodynamic resistance.</p> <p>Pitfall: Relatively highly parameterized hence requires more and accurate crop specific information.</p>

MATERIALS AND METHODS

The algorithms were executed on 10 high resolution airborne images acquired during the Bushland Evapotranspiration and Agricultural Remote Sensing Experiment 2007 and 2008 (BEAREX07 and BEAREX08) field campaign and validated against hourly ET measurements from four large precision weighing lysimeters, two each placed in irrigated and dryland fields. Images were acquired for tall (Corn and Sorghum) and short (Cotton) crops from early to mid-cropping season representing diverse set of agricultural surface roughness with varied land surface energy balance systems.

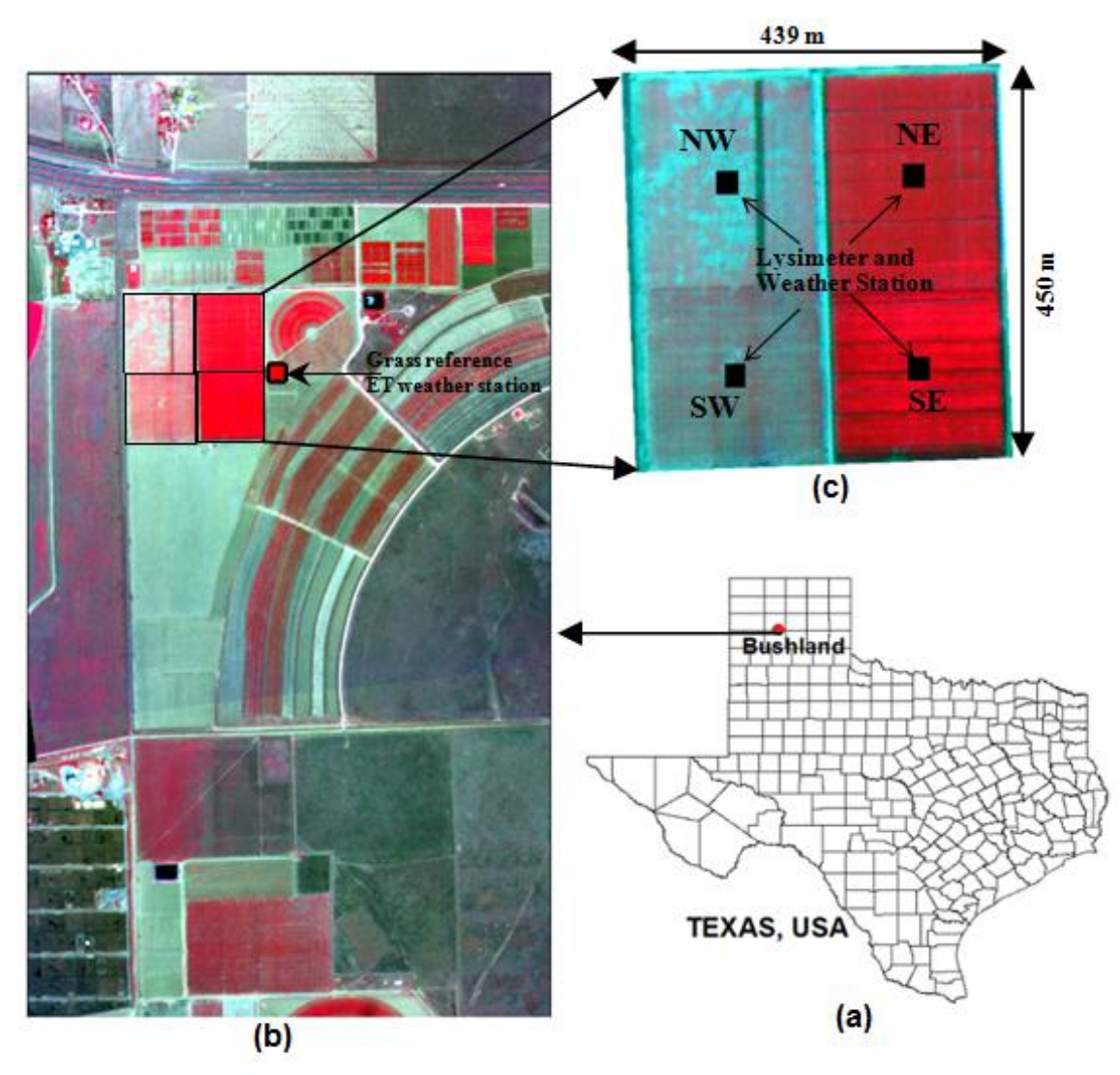


Figure 1: False color composite aircraft image of 5 August, 2008, showing the BEAREX08 study region. (a) location of the study area in reference to the state of Texas, USA; (b) aircraft scene covering a region of close to 5 km²; and (c) exploded view of the lysimeter field.

RESULTS

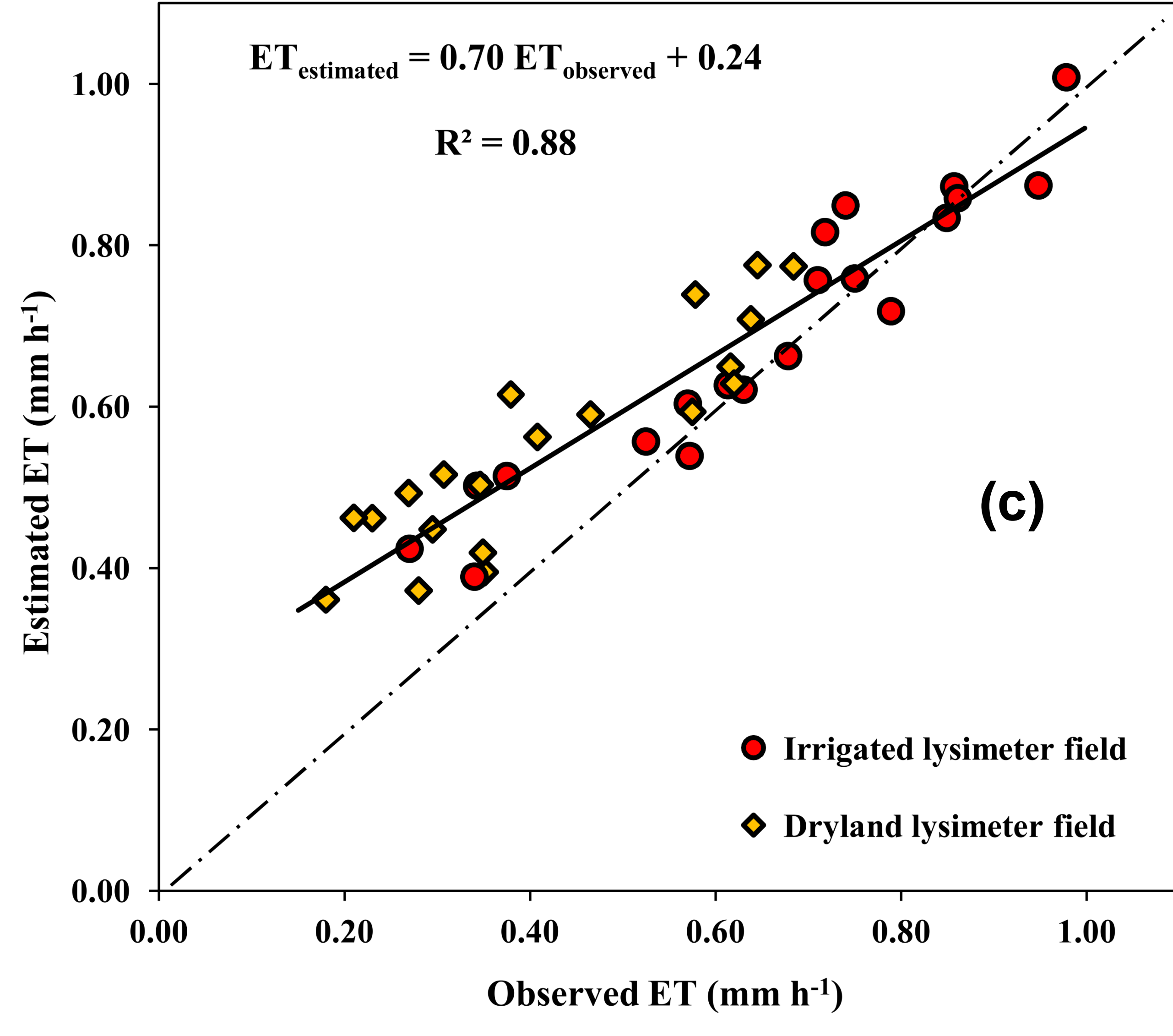
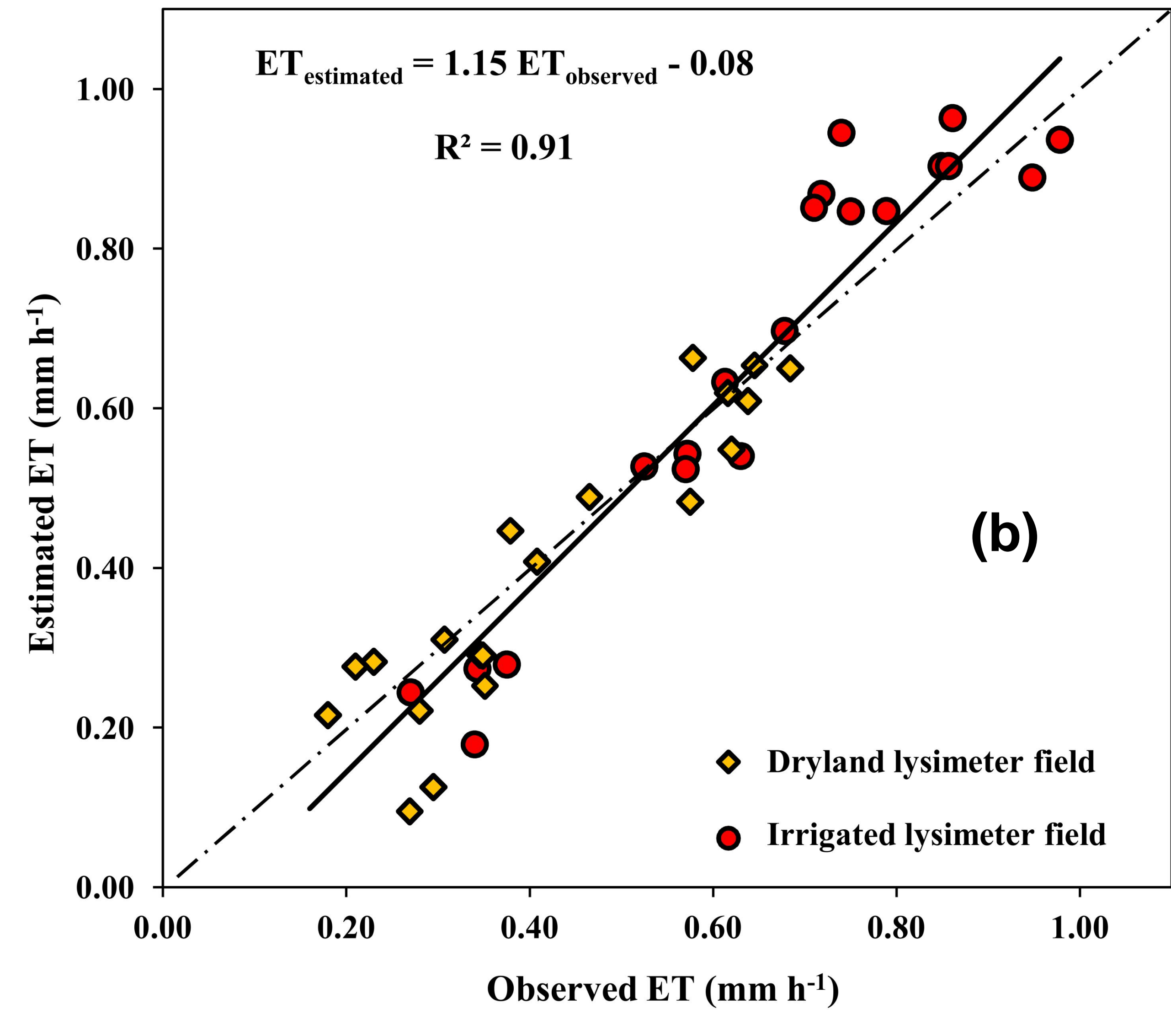
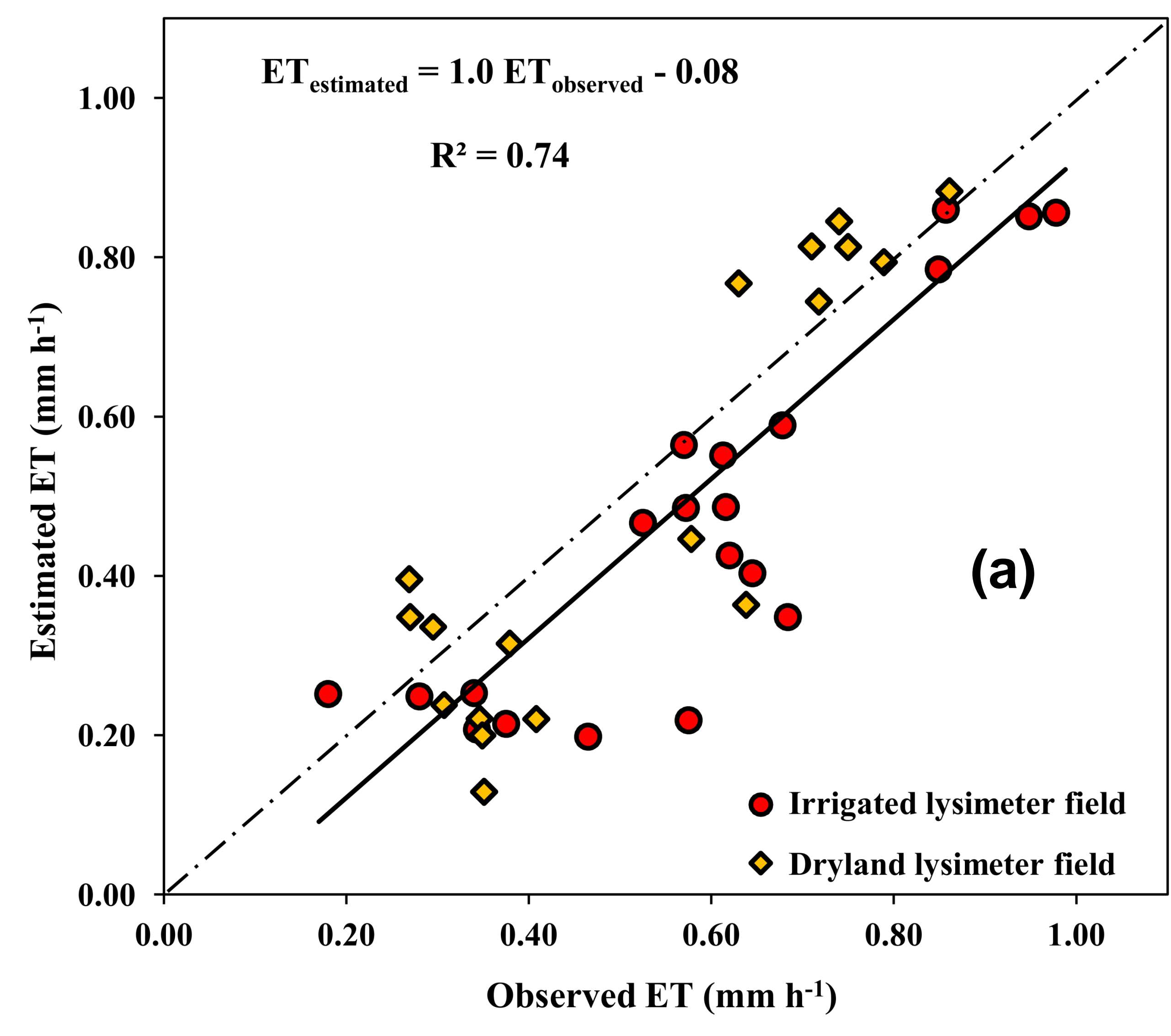


Figure 2: Modeled versus observed ET (a) SEBAL (b) SEBS (c) TSM

Table 1: Performance statistics for T_s (Obs. Mean: 34.6°C), R_n (Obs. Mean: 577), and G_o (Obs. Mean: 37); H (Obs. Mean: 182); (no. of observations = 40).

Estimated parameter	Mean	MBE	%MBE	RMSE	%RMSE	MAE	MAPD	NSE	R ²
T_s (°C)	34.8	0.2	0.7	1.6	4.5	1.1	3.2	0.94	0.95
R_n (W m^{-2})	571	-5.6	-1.0	29.5	5.1	23.5	4.1	0.72	0.76
G_o (W m^{-2})	35	-2.0	-5.3	16.8	45.2	13.2	35.4	0.21	0.23
H_{SEBAL}	228	57.6	33.9	88.7	52.2	72.2	42.5	0.26	0.64
H_{SEBS}	190	8.2	4.5	53.9	29.6	45.2	24.8	0.78	0.83
H_{TSM}	121	-60.7	-33.4	100.5	55.2	83.5	45.8	0.24	0.52

Table 2: Performance statistics for instantaneous ET (mm h^{-1}) for the complete data set, irrigated and dryland fields. Observed mean for the complete dataset, irrigated and dryland fields were 0.54, 0.66 and 0.42 mm h^{-1} respectively.

Models	n	Mean	MBE	%MBE	RMSE	%RMSE	MAE	MAPD	NSE
SEBAL	40*	0.48	-0.08	-14.1	0.14	25.9	0.12	21.5	0.50
	20 [^]	0.63	-0.02	-3.1	0.09	13.4	0.08	11.5	0.81
	20 [^]	0.30	-0.14	-31.8	0.18	41.3	0.17	37.8	-0.55
SEBS	40*	0.53	-0.01	-1.0	0.08	15.7	0.07	12.5	0.85
	20 [^]	0.67	0.01	2.1	0.09	14.1	0.08	11.5	0.79
	20 [^]	0.40	-0.02	-5.9	0.08	18.1	0.06	14.1	0.78
TSM	40*	0.62	0.08	15.1	0.12	22.2	0.09	17.4	0.70
	20 [^]	0.69	0.03	5.1	0.07	11.3	0.05	8.5	0.86
	20 [^]	0.55	0.13	31.4	0.15	36.0	0.13	31.4	0.12

*Complete data, [^]Irrigated fields data, [^]Dryland fields data

SUMMARY

1. Performance statistics for T_s , R_n , and G_o for the complete data set showed good agreement against the measured data.
2. SEBS performance was superior, as evidenced by the smaller error indices and absence of bias error in both dryland and irrigated fields.
3. SEBAL underestimated ET with large variance in the individual errors and poor performance for dryland conditions. TSM overestimated dryland ET and had significant bias error, however, overall performance of TSM was better than SEBAL.

Results suggest that all three models have the potential to be developed as an operational tool for managing water resources by providing accurate and economical spatial ET information.

ACKNOWLEDGMENTS

This research was supported by the Ogallala Aquifer Program, a consortium between USDA-Agricultural Research Service, Kansas State University, Texas A&M AgriLife Research, Texas A&M AgriLife Extension Service, Texas Tech University, and West Texas A&M University. We are grateful to Dr. Christopher M.U. Neale, Professor, Civil and Environmental Engineering, Utah State University for conducting the airborne missions for acquiring the remote sensed imagery.